AD-A151 105 AERODYNAMIC DROPLET BREAKUP(U) SPECTRON DEVELOPMENT 1/1
LABS INC COSTA MESA CA J E CRAIG 02 MAY 83
SDL-83-2193-09 AFOSR-TR-85-0206 F49620-81-C-0032
UNCLASSIFIED F/G 14/2 NL

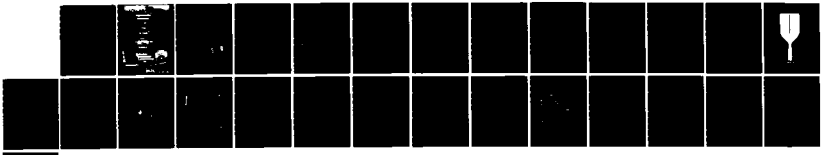

END
FILMED
DTIC

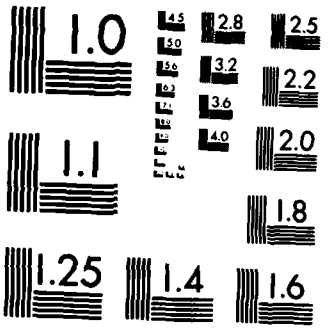

MICROCOPY RESOLUTION TEST CHART
NATIONAL BUREAU OF STANDARDS-1963-A

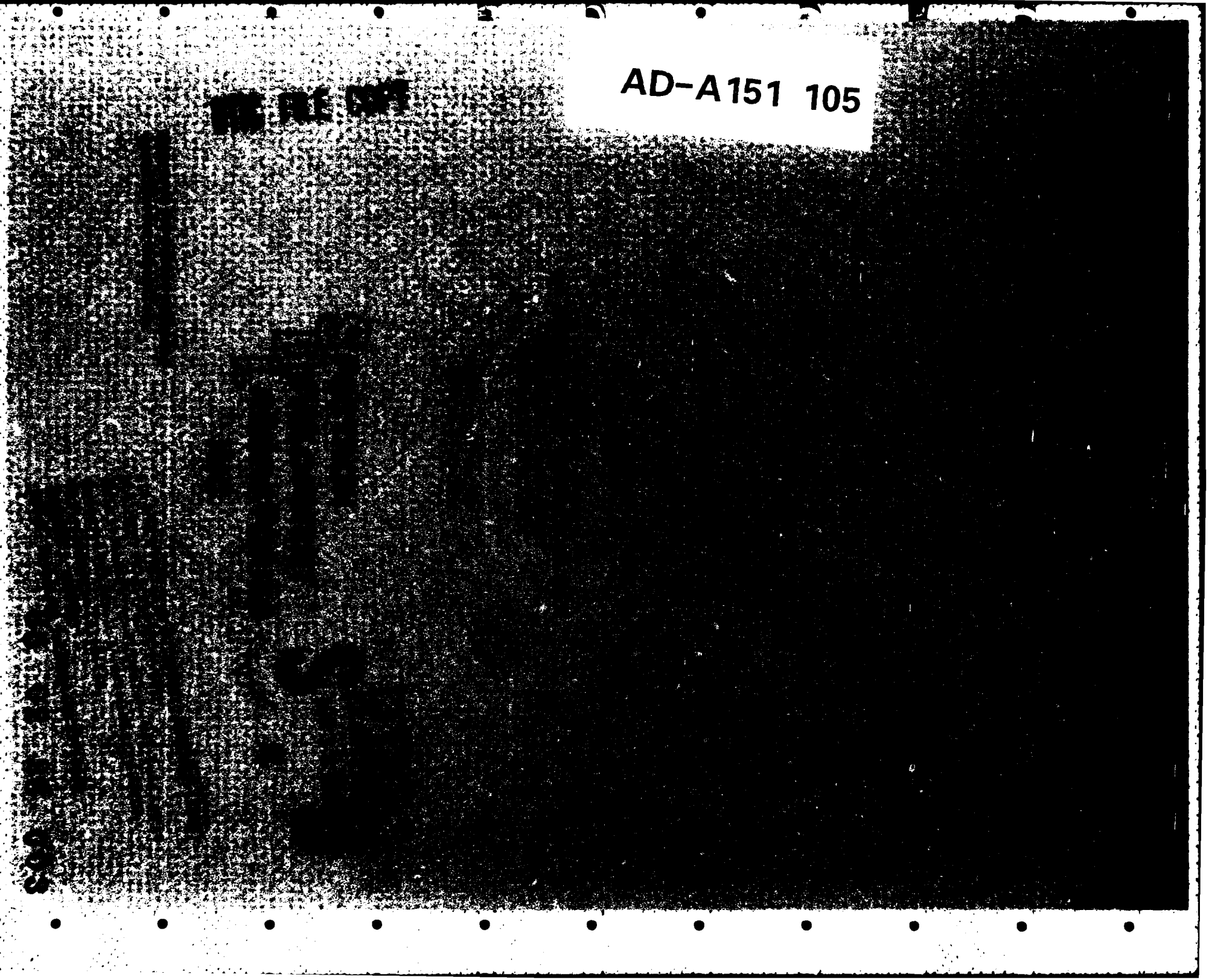

UNCLASSIFIED

SECURITY CLASSIFICATION OF THIS PAGE *(When Data Entered)*

REPORT DOCUMENTATION PAGE	READ INSTRUCTIONS BEFORE COMPLETING FORM
1. REPORT NUMBER: AFOSR-TR- 85-0206	2. GOVT ACCESSION NO: A151105
3. RECIPIENT'S CATALOG NUMBER	
4. TITLE *(and Subtitle)*: AERODYNAMIC DROPLET BREAKUP	5. TYPE OF REPORT & PERIOD COVERED: ANNUAL: 01 FEB 82-30 JAN 83
6. PERFORMING ORG. REPORT NUMBER: SDL No. 83-2193-09	
7. AUTHOR(s): J E Craig	8. CONTRACT OR GRANT NUMBER(s): F49620-81-C-0032
9. PERFORMING ORGANIZATION NAME AND ADDRESS: SPECTRON DEVELOPMENT LABORATORIES, INC. 3303 Harbor Blvd., Suite G-3 Costa Mesa, CA 92626	10. PROGRAM ELEMENT, PROJECT, TASK AREA & WORK UNIT NUMBERS: 61102F 2308/A1
11. CONTROLLING OFFICE NAME AND ADDRESS: AIR FORCE OFFICE OF SCIENTIFIC RESEARCH/NA Building 410, Bolling AFB, DC 20332	12. REPORT DATE: 2 May 1983
	13. NUMBER OF PAGES: 21
14. MONITORING AGENCY NAME & ADDRESS *(if different from Controlling Office)*	15. SECURITY CLASS. *(of this report)*: UNCLASSIFIED
	15a. DECLASSIFICATION DOWNGRADING SCHEDULE

16. DISTRIBUTION STATEMENT *(of this Report)*

Approved for public release; distribution unlimited.

17. DISTRIBUTION STATEMENT *(of the abstract entered in Block 20, if different from Report)*

18. SUPPLEMENTARY NOTES

19. KEY WORDS *(Continue on reverse side if necessary and identify by block number)*

- Droplet Breakup, Fragmentation,
- Droplet Dynamics/Nozzles,
- Scaling Laws: Critical Weber Number, Breakup Time, Fragment Size, and
- Liquid Metals: Mercury, Aluminum.

20. ABSTRACT *(Continue on reverse side if necessary and identify by block number)*

As a result of the previous year's research, we felt that accurate droplet velocity measurements would help us produce scaling laws and provide better interpretation of the holographic droplet images. Therefore, we proceeded with a series of velocimetry experiments designed to provide accurate droplet profile and trajectory data. After completing the velocimetry experiments with conventional liquids, we proceeded with the liquid metals experiments. The results of the velocimetry experiments were reported in the JANNAF paper and will only be summarized here. The experiments with liquid metals are described in detail.

DD FORM 1 JAN 73 1473

UNCLASSIFIED

SECURITY CLASSIFICATION OF THIS PAGE *(When Data Entered)*

AERODYNAMIC DROPLET BREAKUP

ANNUAL TECHNICAL REPORT

J. E. Craig

2 May 1983

SDL No. 83-2193-09

Prepared For:

Dr. Leonard Caveny
AIR FORCE OFFICE OF SCIENTIFIC RESEARCH
Bolling Air Force Base
Washington, D.C. 20332

Under Contract No.
F49620-81-C-0032

SPECTRON DEVELOPMENT LABORATORIES INC.

3303 Harbor Boulevard, Suite G-3
Costa Mesa, California 92626 (714) 549-8477

TABLE OF CONTENTS

LIST OF FIGURES

LIST OF TABLES

SUMMARY - CONVENTIONAL LIQUID EXPERIMENTS

This summary describes the first year's efforts to investigate aerodynamic breakup of conventional liquid droplets. Water, alcohol, and glycerine/water mixtures were selected to provide variation of surface tension and viscosity. A two-dimensional aerodynamic nozzle was configured to subject injected droplets to an aerodynamic load sufficient that droplet breakup would occur within the nozzle contraction. Piezoelectric droplet generators were used to produce highly monodisperse droplets ranging in diameter from 100 to 400 μm. The droplet Weber number, a measure of the ratio of aerodynamic deforming forces to surface tension restoring forces, was established by preselecting droplet size, droplet liquid, and gas velocity. Pulsed laser holography was used to observe the breakup mechanism of liquid droplets and the fragment size distribution. Laser velocimetry was used to determine the droplet and fragment dynamics within the nozzle.

This research has the objective of obtaining physical data to characterize the mechanisms of aerodynamic droplet breakup. The first of a multiphase experiment has been completed in which conventional liquids (water, alcohol, glycerine, etc.) were studied. The primary goal of this initial phase was to examine the effect of liquid properties (viscosity and surface tension) on the breakup mechanism, time scale, and fragment size distribution. The future plans propose to investigate droplets formed from low melting point metals, and finally aluminum and aluminum/aluminum oxide agglomerates.

A key element of the experimental effort is the use of nonintrusive laser diagnostics including pulsed laser holography and laser Doppler velocimetry. The exceptional temporal and spatial resolution of pulsed laser holography provided the ability to resolve the mechanism of breakup and the size distribution of the fragments. Laser Doppler velocimetry was used to determine drop velocity distributions along the nozzle revealing the rapid acceleration of the flattened droplets and then surprisingly the milder acceleration of the fragments. The high drag to mass ratio of the flattened droplets was expected and resolved during the initial phase of the breakup process.

A primary result of the LDV droplet trajectory measurements is the Weber number/breakup time correlation of Figure 1. A two-dimensional nozzle was designed to subject injected droplets to an aerodynamic load sufficient that droplet breakup would occur in the nozzle. The droplet Weber number along its trajectory was calculated for various droplet sizes, liquids and gas velocities. Experiments revealed that rigid droplet trajectory calculations underestimated droplet accelerations prior to breakup. The mechanism for enhanced acceleration was presumed to be droplet flattening, and the result was that droplet Weber numbers were much lower than predicted. Experiment conditions (gas velocity) were adjusted so that droplet breakup occurred, and Weber number histories were determined along the nozzle. The position of maximum Weber number coincided with droplet breakup. This critical Weber number and the associated breakup time are plotted in Figure 1. A breakup zone is identified in which droplet failure occurs for various size droplets, liquid types, and gas velocities.

FIGURE 1.

DROPLET WEBER NUMBER HISTORIES

- CONVENTIONAL LIQUIDS -

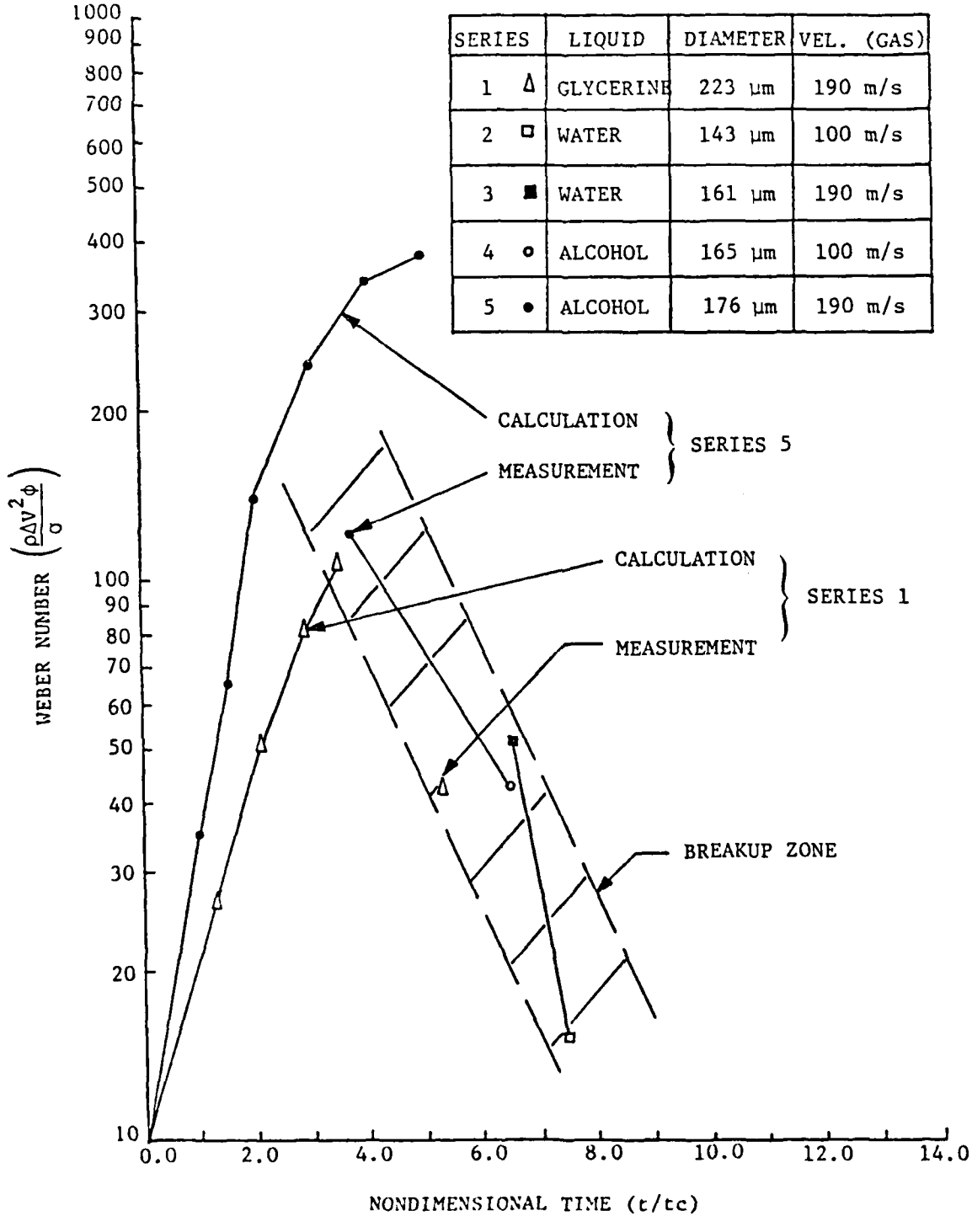

Droplet trajectories were calculated without benefit of the breakup correlation for the final experimental conditions and two are shown in Figure 1. In each case, the peak Weber number is overestimated by about (3X), suggesting that a model for droplet flattening in the drag calculation is appropriate.

The first phase of a three-part experimental investigation of liquid droplet behavior in aerodynamic nozzle contractions has been described. In the initial experiment, conventional liquids have been used to study the effects of two liquid properties; namely, surface tension and viscosity. The dramatic increase in the droplet acceleration caused by flattening was resolved with laser velocimetry. Holographic observation of droplet breakup revealed no substantial differences between breakup resulting from more gradual accelerations in the nozzle contraction and the breakup resulting from instantaneous accelerations in shock tubes. The effect of increased viscosity is to increase the droplet diameter at breakup and to reduce the mean fragment size. Fragment size dependence on Weber number and viscosity was observed.

The second year's effort will concentrate on the breakup dynamics of higher surface tension liquid metal droplets, probably mercury Much of the current technical approach will be used including aerodynamic acceleration, piezoelectric droplet generation, holography and Doppler velocimetry, laser based diagnostics. The nozzle facility will be upgraded to provide supersonic flow required to break up the higher surface tension droplets.

INTRODUCTION

The breakup of AL/AL_2O_3 agglomerates in solid propellant rocket nozzles is a critical process effecting combustion efficiency and two-phase flow losses. While direct observation of agglomerate breakup has been made in subscale nozzles, the dynamics and mechanisms of breakup remain to be characterized. These phenomena for high suface tension metal droplets may differ significantly from those associated with conventional liquid droplets. Proper scientific scaling techniques must be developed to extrapolate subscale laboratory data to full scale rocket motor pressures, temperatures, and sizes. The principle goal of this investigation is to provide increased understanding of the fundamental breakup mechanisms of high surface tension AL/AL_2O_3 agglomerates in aerodynamic nozzles.

Droplet breakup experiments in aerodynamic nozzle contractions have been conducted in which conventional liquids and higher surface tension liquids (Mercury) were examined. A key element of the experiment is the use of laser diagnostics. Pulsed laser holography has provided droplet and fragment observations with resolutions not previously possible. Laser velocimetry has provided droplet dynamics data revealing dramatic accelerations prior to breakup.

EXPERIMENT DESIGN

A series of experiments were designed to investigate the breakup dynamics of high surface tension liquid metals. Many liquid metals were identified, but mercury was selected as it was compatible with the droplet generation, the technique, and with room temperature air experiments. The aerodynamics of the experiment were based on trajectory estimates for mercury droplets from 100 to 600 μm. Since the liquid-to-gas density ratio was so large, the droplet velocities were assumed to be small and the slip velocity was taken as the gas velocity. This fact was verified in the experiments when the droplet velocity limited to less than 10 percent of the gas velocity. The slip velocity or gas velocity requirement ranged from 270 m/s to 109 m/s for droplet diameters of 100 μm to 600 μm, respectively. Therefore, we decided to do one series of experiments with the nozzle choked in which the droplet size would be varied.

The 2-dimensional nozzle facility was modified to achieve sonic velocity in the throat (Figure 2). The nozzle would start and was operated at a stagnation pressure of 27 psia. A droplet generator with a 130 μm diameter orifice was operated at 10 kHz and 1.5 kHz, to produce 190 μm and 300 μm diameter droplets, respectively; and a second orifice size (ϕ = 190 μm) was operated at 840 Hz to produce 560 μm diameter droplets. The test matrix is shown in Table 1. The pulsed laser holography was used to record droplet images in various states along the nozzle.

FIGURE 2.

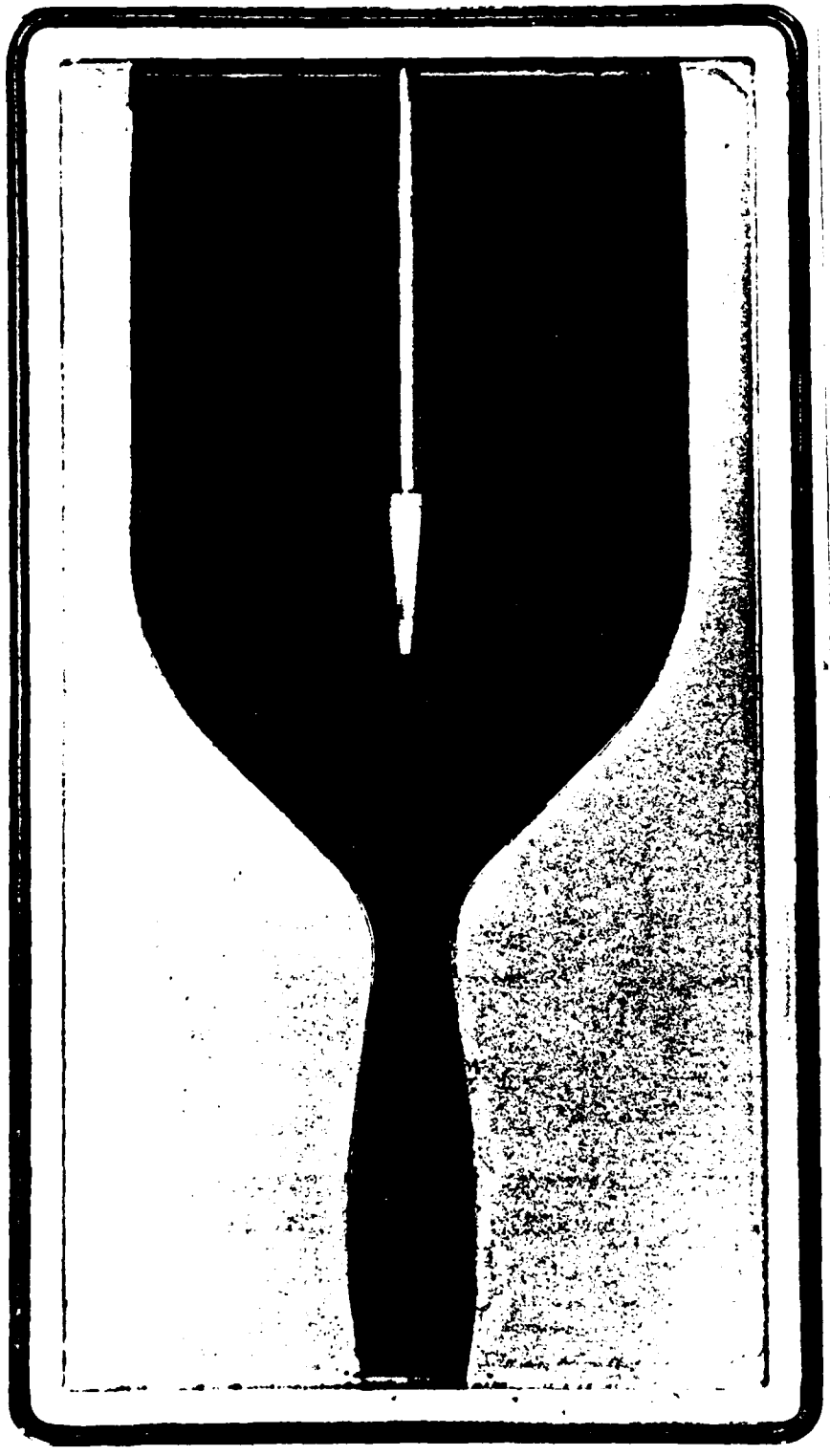

SUPERSONIC DROPLET BREAKUP NOZZLE

DROPLET BREAKUP SCALING

CONDITIONS	LABORATORY BREAKUP SCALING			FULL SCALE PREDICTIONS
	CONVENTIONAL LIQUIDS	MERCURY	ALUMINUM	
GAS				
PRESSURE (ATM)	1.0	2.0	38.0	70.0
VELOCITY (M/S)	100.0	300.0	100.0	1000.0
THROAT SIZE (CM)	1.0	1.0	0.3	10.0
TEMPERATURE (°K)	300.0	300.0	2500.0	3200.0
DROPLET				
SURFACE TENSION (DYN/CM)	50.0	460.0	850.0	850.0
DENSITY (GM/CM^3)	1.0	13.5	2.4	2.4
DYNAMICS				
LIQUID/GAS DENSITY RATIO	770.0	7000.0	400.0	281.0
LIQUID/GAS VELOCITY RATIO				
MEASURED	0.5	0.1	0.1	-
PREDICTED	0.1	0.1	-	0.3
BREAKUP				
MINIMUM SIZE				
MEASURED (μM)	250.0	100.0	500.0	
PREDICTED (μM)	100.0	100.0	-	< 200.0

83-2193-09/D9

DISCUSSION

The trajectory data obtained for low density conventional liquids ($\rho_L/\rho_g \simeq 770$) reveals droplet velocities which are sizable fractions of the gas velocity (say 20-40 percent); whereas the holographic data for the high density liquid, mercury ($\rho_L/\rho_g = 7000$) reveals droplet velocities which never exceed 10 percent of the gas velocity. We expected that the droplet accelerations would be higher for lower density ratios. We emphasize the point because, for the rocket motor case with aluminum droplets, the density ratio ($\rho_L/\rho_g \simeq 200$) is lower than any condition achieved in these experiments, as shown in Table 2. Therefore, dynamics calculations are required to predict droplet/gas slip velocity, Weber number, or droplet breakup.

The conditions for droplet breakup appear to be different for conventional liquids than for liquid metals. The Weber number and breakup time correlations developed for conventional liquids indicate that in some conditions droplets survive to Weber numbers exceeding 100, and in other conditions, breaking occurs at lower Weber numbers. The liquid metal data shows that with proper scaling a complete set of data collapse to one curve. Droplet breakup occurs when the Weber number exceeds 15 or 20 and when the nondimensional time exceeds one. The liquid metal data reveal scaling techniques not exhibited in the conventional liquid data. We plan to obtain holography data for the conventional liquid droplets in a series of experiments much like the mercury droplet experiments, where, for fixed gas speed, the droplet size was varied. The liquids used in these experiments will be water, alcohol, and water/glycerine mixtures.

and it is not at all clear how this situation changes if the number density of the incident droplets increases significantly.

FIGURE 8.

EQUILIBRIUM FRAGMENT NUMBER DENSITY DISTRIBUTION

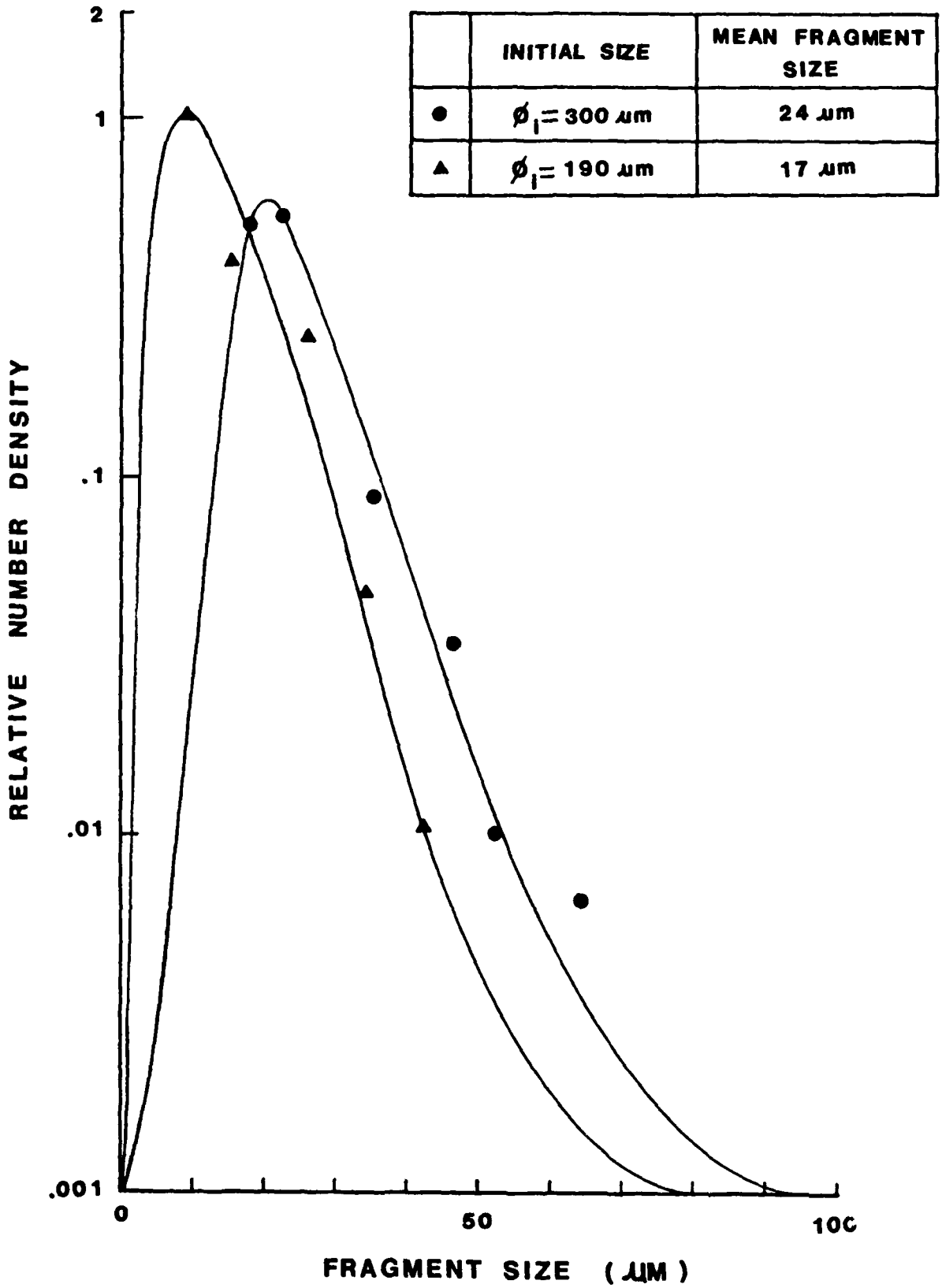

FIGURE 7.

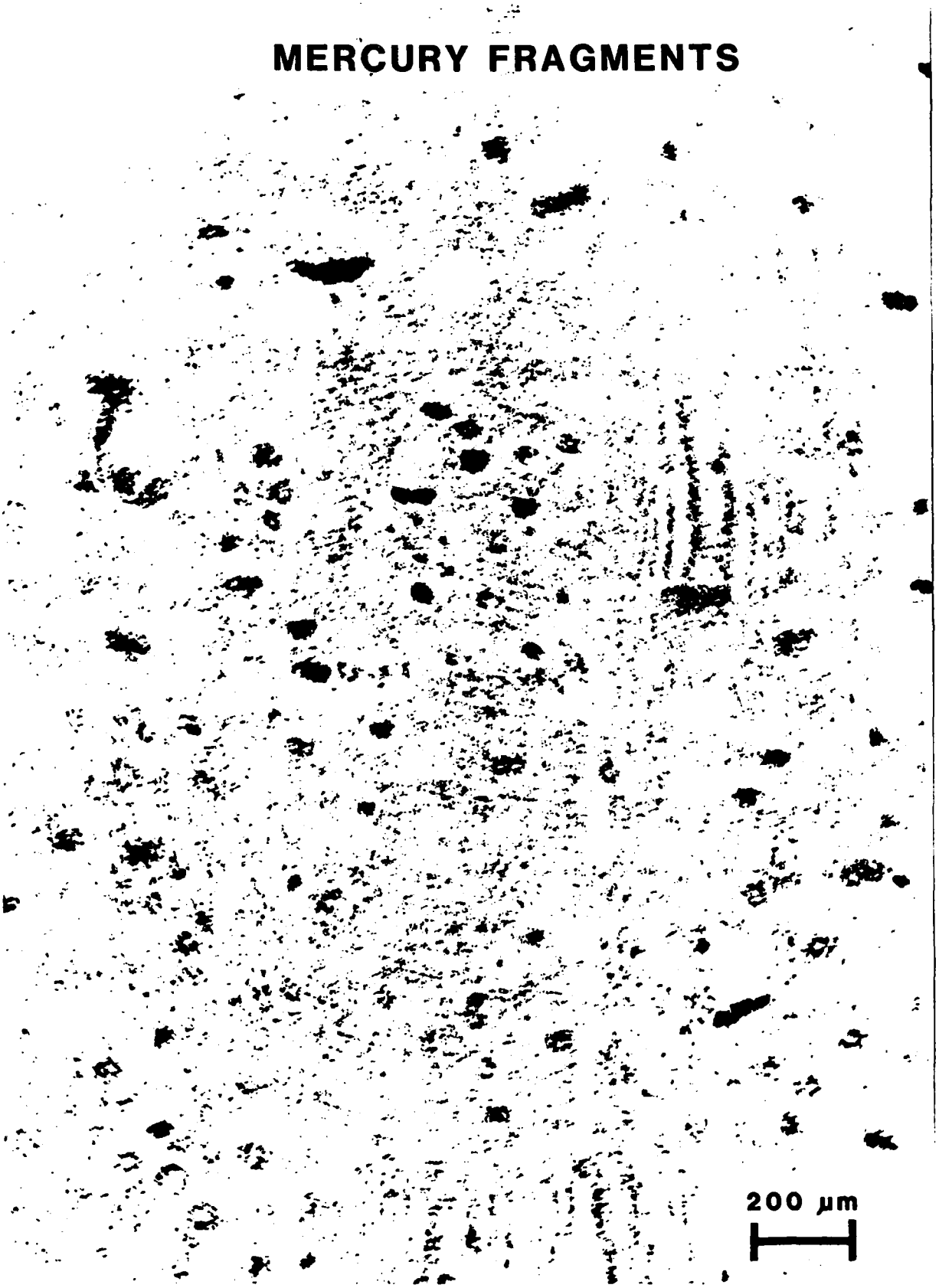

FIGURE 6.

DROPLET WEBER NUMBER HISTORIES

MERCURY

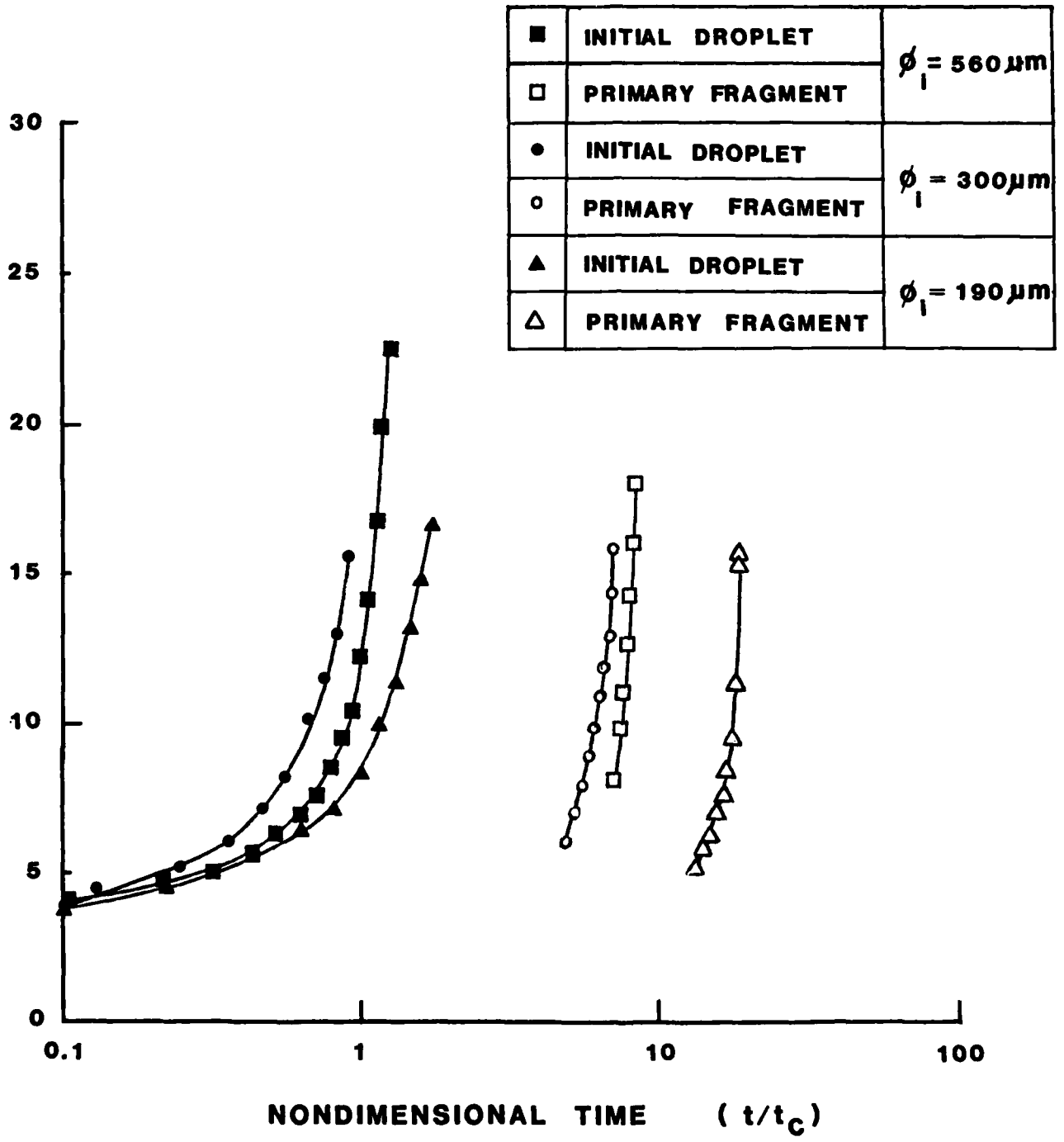

DROPLET VELOCITY AND WEBER NUMBER PROFILES

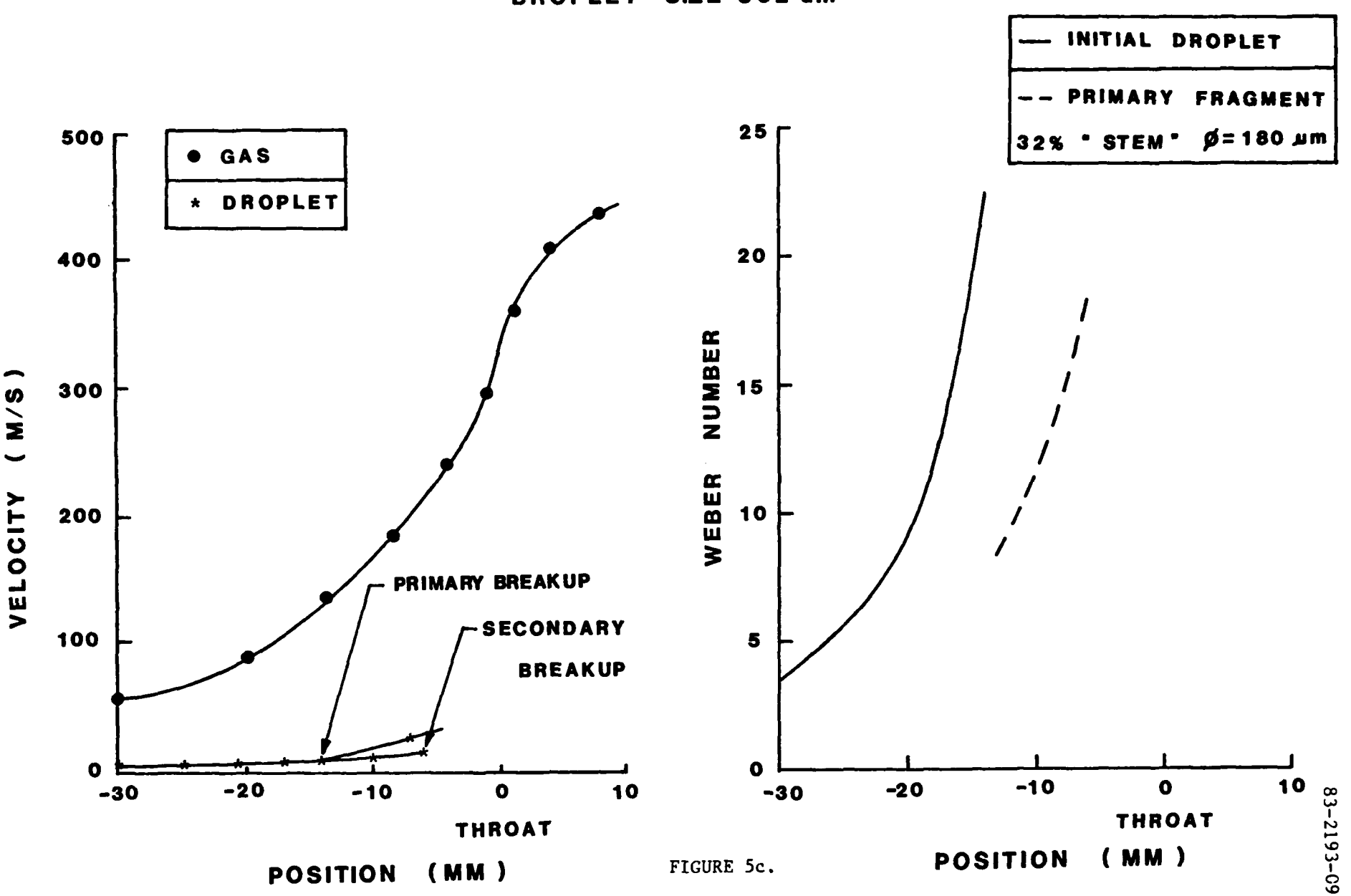

FIGURE 5c.

DROPLET VELOCITY AND WEBER NUMBER PROFILES

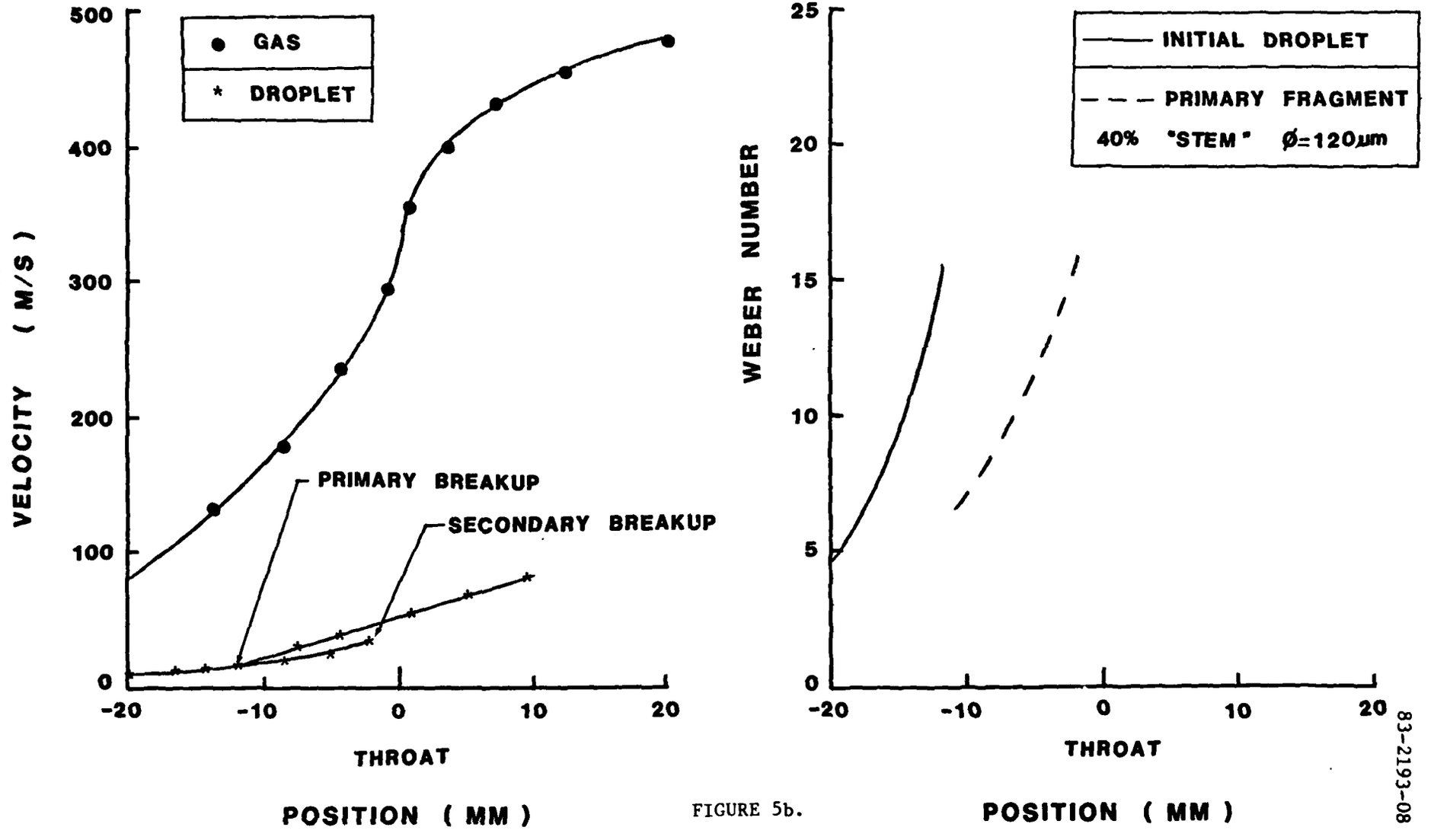

FIGURE 5b.

DROPLET VELOCITY AND WEBER NUMBER PROFILES

DROPLET SIZE = 190 μm

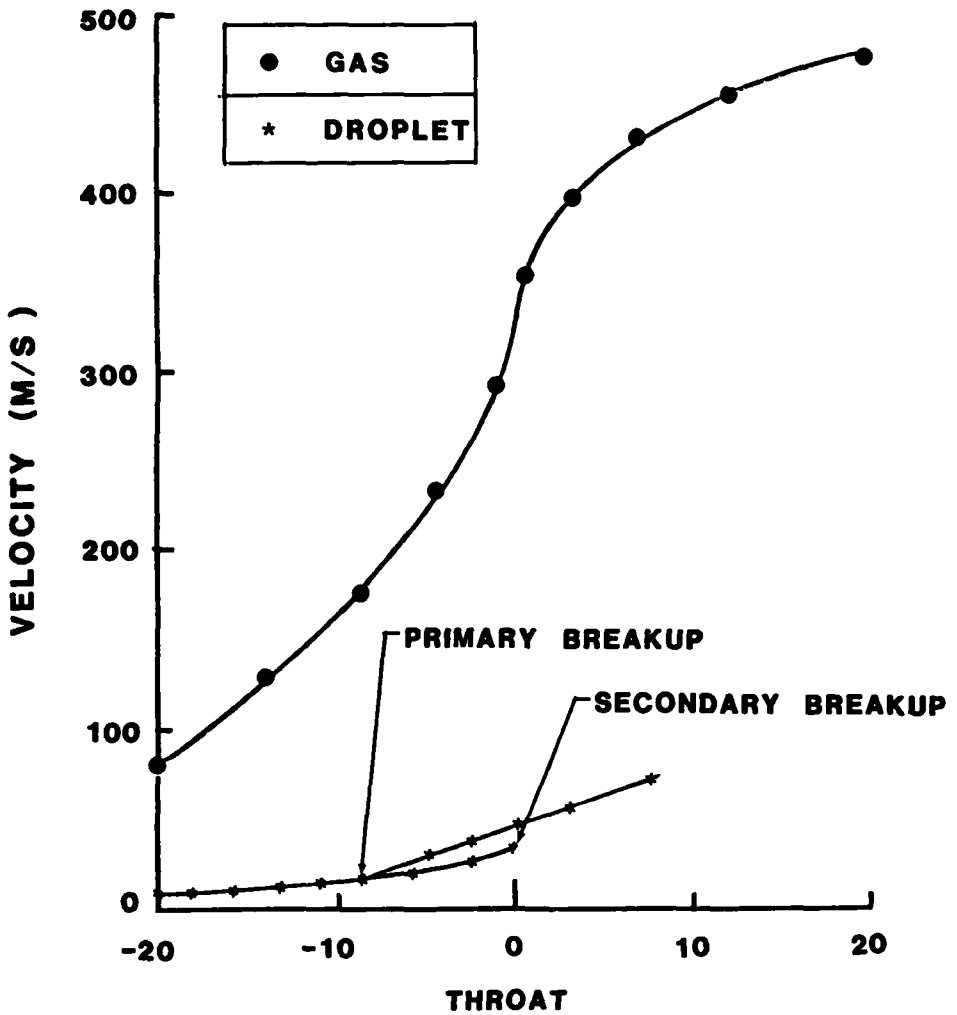

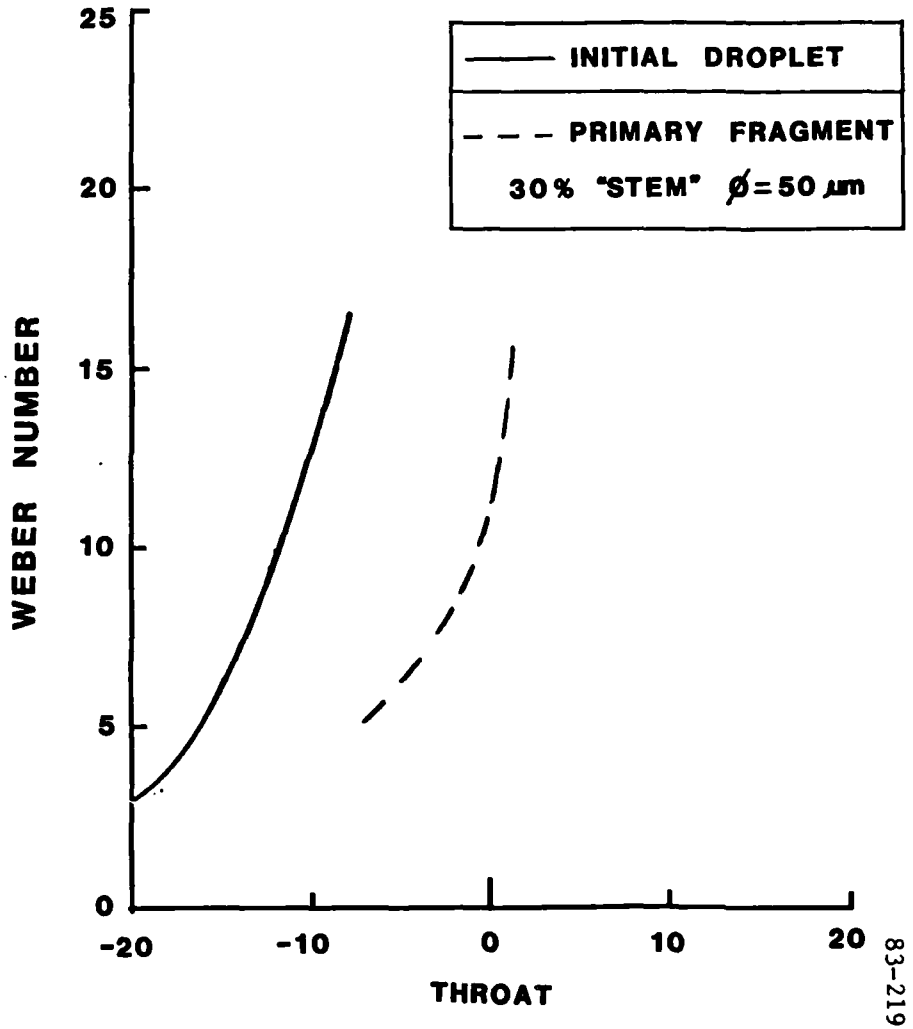

FIGURE 5a.

83-2193-08

smaller fragments are spherical. The larger fragments arise from the stem and ring and the smaller fragments arise from the sheet.

The velocity and Weber number profiles (Figure 5) depict the velocity of the initial droplet, the primary fragments, and the stem. The position (upstream of the throat) for the primary breakup moves from 8.0 mm to 14.0 mm for the initial droplet-sizes 190 μm to 560 μm, respectively.

The Weber number is based on the slip velocity and initial droplet size; then, for the stem, the Weber number is based on an approximate frontal diameter (typically $\phi_s \simeq .30\ \phi_o$). All primary droplets fall in the Weber number range of 15-20, and the stems fall in a similar range. The Weber number histories (Figure 6) of all three sizes overlap to within the accuracy of the data, when the time is normalized by the period of the first natural frequency $t \simeq \left(\frac{\rho\phi^3}{\sigma}\right)^{1/2}$. This period for acoustic oscillation and the breakup time are essentially equivalent. This result is in striking contrast to the result obtained for conventional liquids for which the Weber number and breakup time varied with droplet diamter and gas velocity.

The fragment size distribution was determined from high magnification photographs (Figure 7). An estimate of the equivalent spherical diameter was used for nonspherical fragments. The fragment number density distribution (Figure 8) ranges from 5-50 μm and the sampling volume for each droplet size bin is corrected for the depth of field. For all three initial droplet sizes, the mean fragment size is about 10 percent of the original droplet diameter. Note here that the fragment number density distribution arises from the breakup of a single droplet,

FIGURE 4.

PRIMARY FRAGMENTATION PROCESS

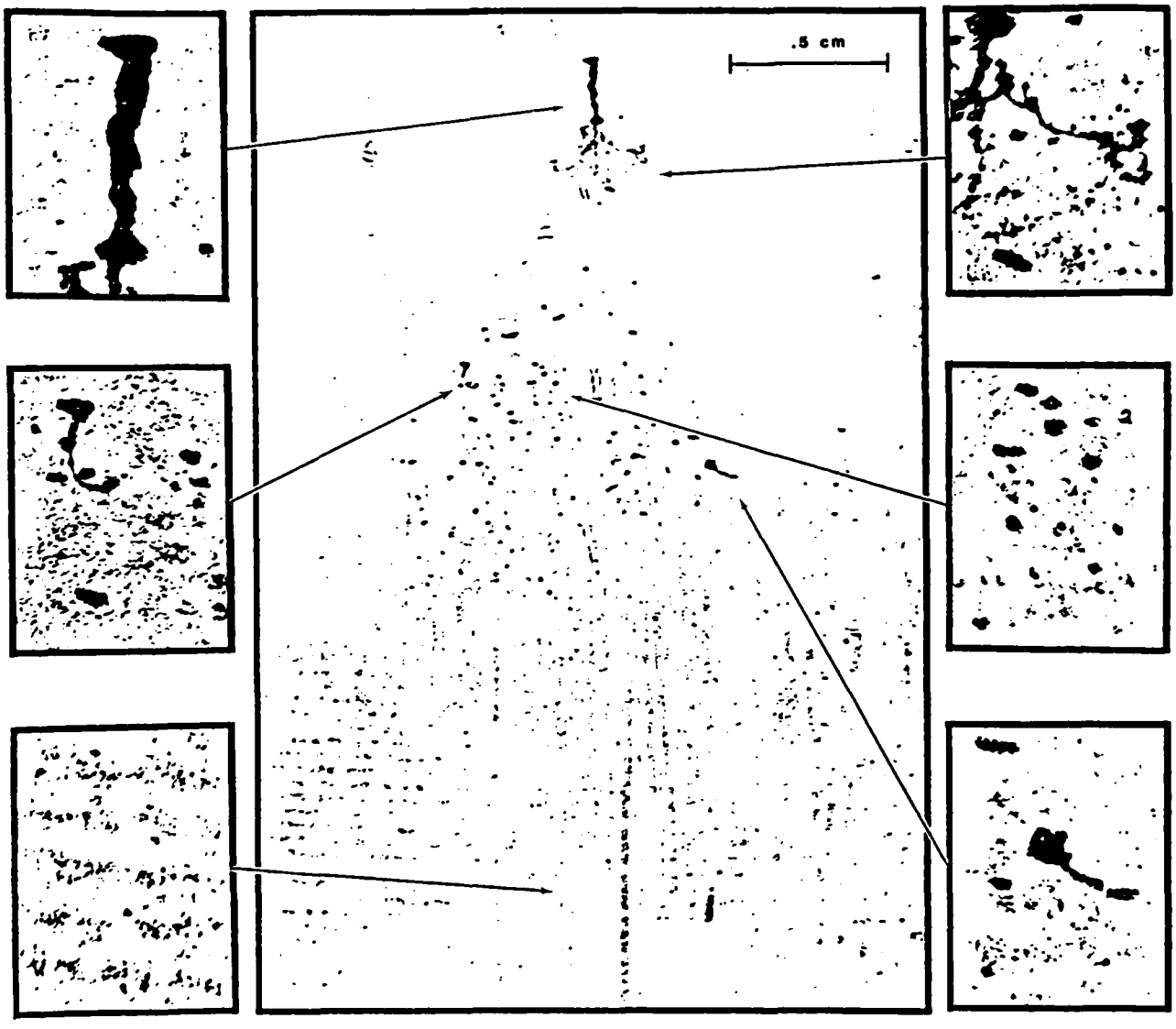

FIGURE 3.

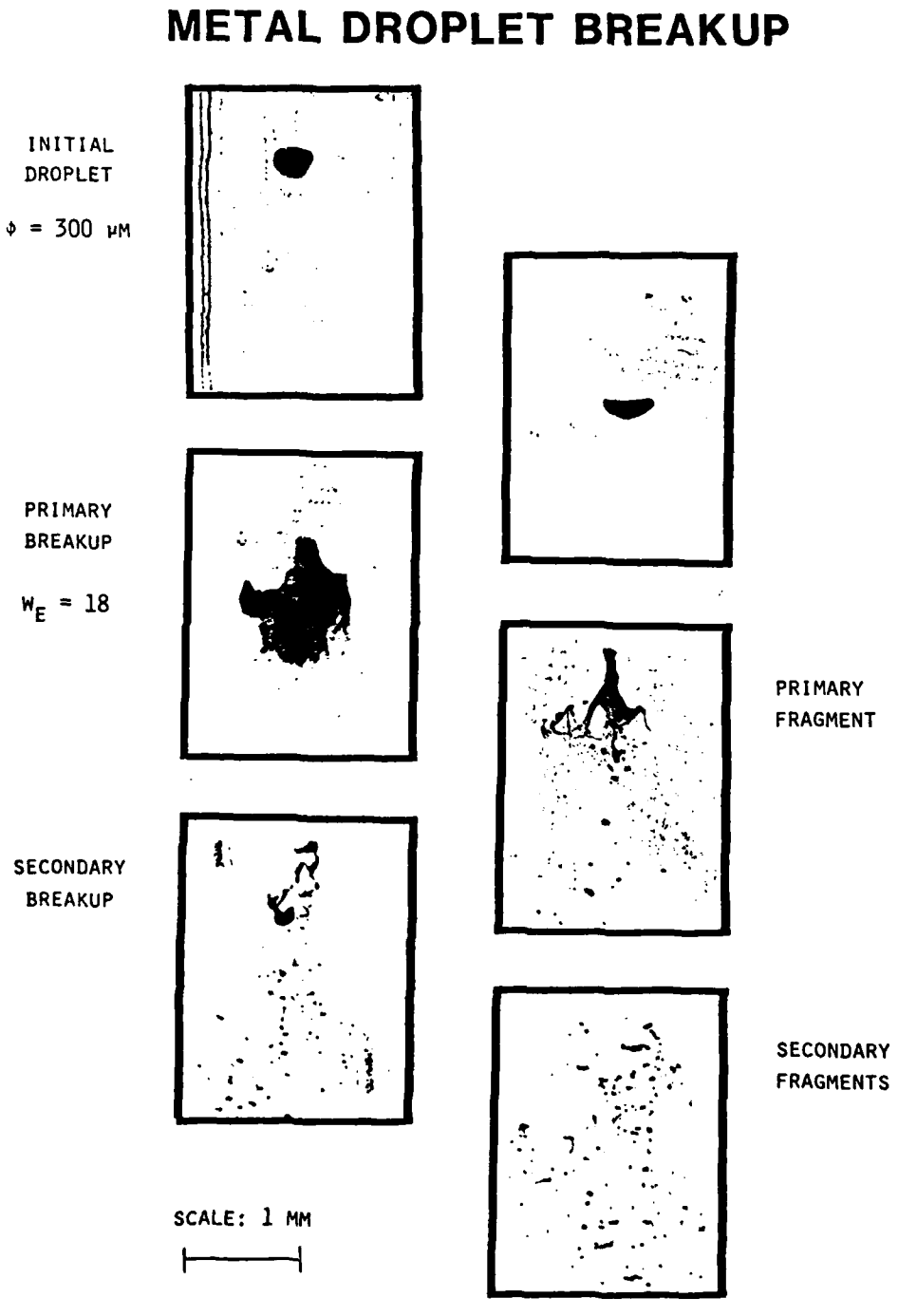
METAL DROPLET BREAKUP
INITIAL DROPLET
ϕ = 300 μM
PRIMARY BREAKUP
W_E = 18
SECONDARY BREAKUP
PRIMARY FRAGMENT
SECONDARY FRAGMENTS
SCALE: 1 MM

RESULTS

The droplet breakup process was very similar for the three droplet sizes, except that the breakup moved to a higher gas velocity position in the nozzle for smaller droplets. The breakup mechanism (Figure 3) is observed to be the Umbrella Mode characteristic of the Weber number range of 70-100 for conventional liquids. In this breakup mode, the droplets initially flatten and then almost explode to much larger dimensions (3-5X) forming the stem in the center and a sheet between the stem and the outer ring. The sheet bursts very quickly constituting the primary breakup event. The outer ring fragments soon after the sheet bursts. The stem is very stable at this point and remains secure until a higher slip velocity is reached. The sheet and ring fragments are much smaller and accelerate away from the massive stem (Figure 4). The stem is rather cylindrical and aligned with the flow. The frontal diameter of the stem is about 30-40 percent of the original droplet size and begins to deform as higher velocities are reached in the nozzle.

Secondary breakup (Figure 3) is observed as the stem approaches the throat. The Weber number for secondary breakup, based on original stem diameter (i.e., 30% ϕ_o), is in the 10-20 range. The primary fragments travel downstream of the stem during the secondary breakup cycle, and at the throat the most distant fragments (which are also the smallest) are about 2.5 cm downstream of the stem. Finally, after the stem has failed, the breakup is essentially complete and most of the

TABLE 1

TEST MATRIX MERCURY DROPLETS

GAS VELOCITY (m/s)	DROPLET SIZE (μm)	DROPLET VELOCITY (m/s)	SLIP VELOCITY (m/s)	WEBER NUMBER
310	190	19	197	16.5
310	300	17	154	17.9
310	562	9.5	119	22.6
175	436	8.1	153	28.8

Mercury Liquid Properties:

Density - 13.55 gm/cm^3

Surface Tension - 465 dyne/cm

Viscosity - 1.55 centipoise

END

FILMED

4-85

DTIC